Absence of mobility edges in mosaic Wannier-Stark lattices

Stefano Longhi *

Dipartimento di Fisica, Politecnico di Milano, Piazza L. da Vinci 32, I-20133 Milano, Italy and IFISC (UIB-CSIC), Instituto de Fisica Interdisciplinar y Sistemas Complejos, E-07122 Palma de Mallorca, Spain

(Received 21 July 2023; revised 9 August 2023; accepted 9 August 2023; published 21 August 2023)

Mobility edges, separating localized from extended states, are known to arise in the single-particle energy spectrum of certain one-dimensional models with quasiperiodic disorder. Recently, some works claimed rather unexpectedly that mobility edges can exist even in disorder-free one-dimensional models, suggesting as an example the so-called mosaic Wannier-Stark lattice where a Stark potential is applied on every M site of the lattice. Here, we present an exact spectral analysis of the mosaic Wannier-Stark Hamiltonian and prove that, strictly speaking, there are not mobility edges, separating extended and localized states. Specifically, we prove that the energy spectrum is almost pure point with all the wave functions displaying a higher than exponential localization with the exception of $(M-1)$-isolated extended states at energies around which a countably infinite number of localized states with a diverging localization size condense.

DOI: 10.1103/PhysRevB.108.064206

I. INTRODUCTION

Anderson localization [1–4], i.e., the inhibition of wave diffusion in disordered media via destructive interference of multiply scattered waves is a universal phenomenon observed in a variety of classical and quantum systems with experimental demonstrations reported in different areas of physics ranging from photonics [5–7], acoustics [8], matter waves [9–13], and quantum matter [14], to mention a few. The kind of disorder and the spatial dimension of the system are pivotal to Anderson localization since they strongly affect the appearance of localization transitions and the existence of mobility edges [2–4,15–17], i.e., critical energies separating extended and localized states in the spectrum. In low-dimensional systems with uncorrelated disorder, localization transitions and mobility edges are prevented [4,15]. Conversely, quasiperiodic systems, i.e., quasicrystals, can show localization transitions and mobility edges even in one-spatial dimension (see, e.g., Refs. [18–32] and references therein). Quasiperiodic models displaying mobility edges include special incommensurate potentials displaying a generalized Aubry-André self-duality [20–22], slowly varying incommensurate potentials [18,23–28], flat-band lattices [29], and quasiperiodic mosaic lattices [30], to mention a few. A different form of mobility edges, separating localized and critical (rather than extended) wave functions, has been also predicted and experimentally observed in certain quasiperiodic potentials [33–40].

Recently, some works suggested that mobility edges can exist in models without disorder nor incommensurate potentials, i.e., in disorder-free systems [41–43]. Specifically, they considered the so-called mosaic Wannier-Stark lattice, i.e., a lattice in which a Stark (linear gradient) potential is applied at every M sites in the lattice. For $M = 1$, the Hamiltonian shows a pure point spectrum, the Wannier-Stark ladder energy spectrum, with localized wave functions and a corresponding periodic dynamics in the time domain (the famous Bloch oscillations) [44–47]. However, when $M \geqslant 2$ mobility edges are claimed to arise, the coexistence of extended states and Wannier-Stark localized states in the energy spectrum. This is a rather puzzling claim given the system has no disorder nor quasiperiodicity and motivates investigating the nature of the eigenstates of the mosaic Wannier-Stark Hamiltonian carefully.

In this paper, we present an exact analytical solution to the mosaic Wannier-Stark model and show that the energy spectrum is almost pure point and, thus, strictly speaking, there are not mobility edges. Specifically, we show that all eigenfunctions are localized with a higher than exponential localization with the exception of $(M-1)$-isolated extended states. The localized eigenfunctions can be classified into two sets: high-energy wave functions with energies outside the lattice band, and low-energy wave functions with energies inside the lattice band. The eigenenergies of the low-energy wave functions condense toward the energies of the isolated extended states, whereas, the energies of the high-energy wave functions are unbounded and approximate the usual Wannier-Stark ladder in the high-energy limit. Although the high-energy wave functions are tightly localized in very few sites of the lattice, the low-energy wave functions can extend over a large size w of the lattice, however, asymptotically, they decay faster than any exponential and, thus, they are normalizable wave functions belonging to the point spectrum of the Hamiltonian. However, as the energy E of the localized wave function approaches one of the $(M-1)$-isolated energies of thee extended states, the localization size w diverges.

II. MOSAIC WANNIER-STARK HAMILTONIAN: MODEL AND ENERGY SPECTRUM

The spectral properties of the disorder-free mosaic Wannier-Stark lattice [41–43] are defined by the eigenvalue

*stefano.longhi@polimi.it

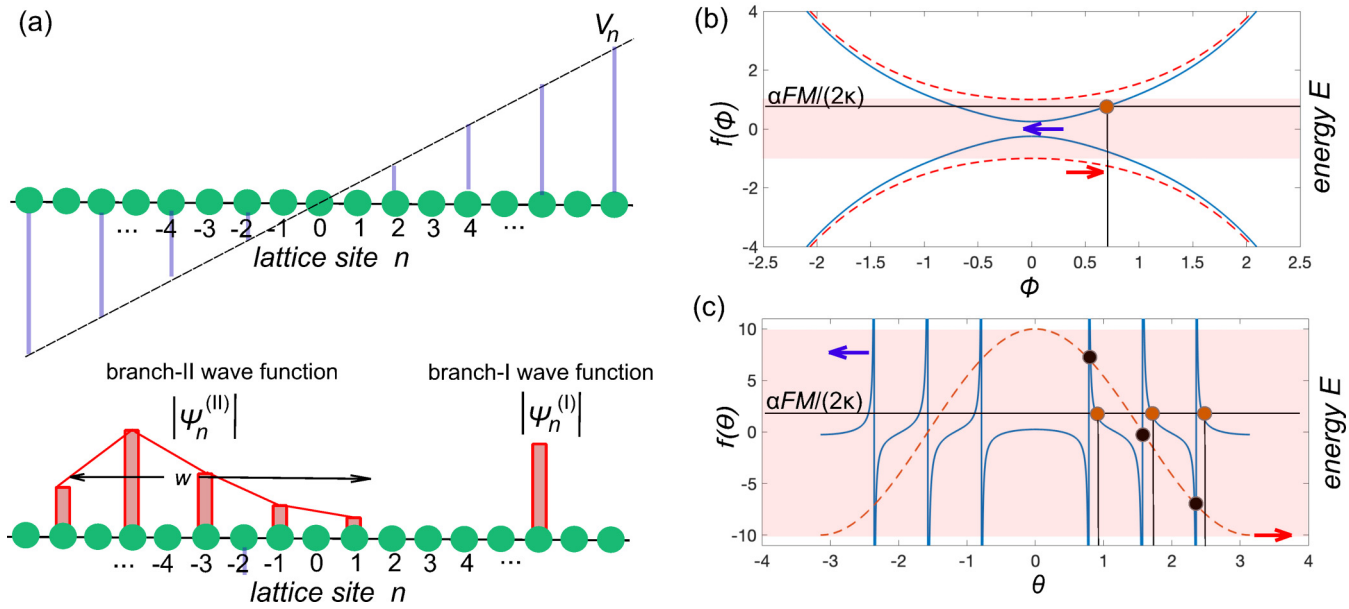

FIG. 1. (a) Schematic of the Wannier-Stark mosaic lattice. A linear gradient potential $V_n = nF$ is applied at every M sites of the lattice ($M = 2$ in the figure). The wave functions are mostly localized either in the lattice sites with nonvanishing potential (branch I) or in the lattice sites with the vanishing potential (branch II). A wave function belonging to branch I is tightly localized at around one single site of the lattice with $V_n \neq 0$, whereas, a wave function of branch II is weakly localized and can extend over several sites with a localization length w, which diverges as its eigenenergy approaches one of the $(M-1)$ values E_σ. (b) and (c) Geometric solution to Eqs. (7) and (9) for the calculation of the energy spectra $E_\alpha^{(I)}$ and $E_\alpha^{(II)}$ of the two branches. Panel (b) shows the behavior of the function $f(\phi) = \pm \sinh\,\phi\,\cosh(M\phi)/\sinh(M\phi)$ (solid blue curves) for $M = 4$ and energies $E = \pm 2\kappa\,\cosh\,\phi$ (dashed red curves). The horizontal solid line yields the quantized value $\alpha F/(2\kappa)$ with an α integer. The bold circle corresponds to the simple positive root ϕ to Eq. (7). (c) The same as (b) but with $f(\theta) = \sin\,\theta\,\cos(M\theta)/\sin(M\theta)$. The three bold red circles correspond to the $(M-1) = 3$ positive roots θ to Eq. (9) in the range of $(0, \pi)$, which are denoted by the additional index $\rho = 1, 2, \ldots, M-1$. The solid black circles in (c), at which $f(\theta)$ is singular, correspond to the $(M-1)$ energies E_σ of extended states. The shaded light areas in (b) and (c) denote the energy interval $(-2\kappa, 2\kappa)$ of the tight-binding lattice in the absence of the potential. Note that in (b), any energy belonging to $E_\alpha^{(I)}$ falls outside the shaded area, whereas, in (c), any energy belonging to $E_\alpha^{(II)}$ falls inside the shaded area.

equation,

$$E\psi_n = \kappa(\psi_{n+1} + \psi_{n-1}) + V_n\psi_n \equiv \mathcal{H}\psi_n, \tag{1}$$

where κ is the hopping amplitude between adjacent sites in the lattice and V_n is the Stark potential, applied at every M site of the lattice, i.e.,

$$V_n = \begin{cases} Fn, & n = 0, \pm M, \pm 2M, \pm 3M, \ldots \\ 0, & \text{otherwise}, \end{cases} \tag{2}$$

and F is the force. A schematic of the mosaic Wannier-Stark lattice is displayed in Fig. 1(a). For $M = 1$, one recovers the famous Wannier-Stark problem of a quantum particle hopping on a one-dimensional lattice subjected to a DC force F. This problem is exactly solvable, and the Hamiltonian $\mathcal{H}$ displays a pure point energy spectrum with equally spaced energies $E_\alpha = \alpha F$ ($\alpha = 0, \pm 1, \pm 2, \pm 3, \ldots$) forming the Wannier-Stark ladder and yielding in the time domain a periodic motion of the wave packet (Bloch oscillations [44–47]). The corresponding wave functions are the well-known Wannier-Stark states, which are given in terms of Bessel functions of the first kind,

$$\psi_n^{(\alpha)} = (-1)^{n-\alpha} J_{n-\alpha}(2\kappa/F), \tag{3}$$

and show a higher than exponential localization, i.e., $\lim_{n\to\pm\infty} \psi_n^{(\alpha)} \exp(R|n|) = 0$ for any $R \geqslant 0$.

Here, we provide exact analytical results on the energy spectrum and corresponding eigenfunctions for the mosaic Wannier-Stark Hamiltonian when $M \geqslant 2$. According to the Simon-Spencer theorem [48] since the potential V_n is unbounded at infinity, the absolutely continuous part of the energy spectrum of $\mathcal{H}$ is empty, i.e., the energy spectrum comprises pure point and/or singular continuous parts. The Simon-Spencer theorem basically excludes the existence of bands of extended states for the mosaic Wannier-Stark Hamiltonian, and the corresponding eigenfunctions, therefore, should be either normalizable (localized) states or critical states. However, the Simon-Spencer theorem does not exclude the existence of isolated extended states with zero spectral measure of the corresponding energies. This means that, if mobility edges would exist, they should separate localized and critical states. The main result of the present paper is that the energy spectrum is almost pure point, and there are not mobility edges. The results are summarized by the following *theorem*:

(1) The energy spectrum of $\mathcal{H}$ on the infinitely extended lattice and for $M \geqslant 2$ is pure point with corresponding eigenfunctions displaying a higher than exponential localization with the exception of $(M-1)$-isolated energies, given by

$$E_\sigma = 2\kappa\,\cos\left(\frac{\pi\sigma}{M}\right), \tag{4}$$

($\sigma = 1, 2, \ldots, M-1$) at which the corresponding eigenfunctions are the following non-normalizable (improper) extended

states:

$$\psi_n^{(\sigma)} = \sin(n\pi\sigma/M). \tag{5}$$

(2) The eigenenergies of the localized wave functions can be grouped into two sets: the high-energy wave functions (set I) and the low-energy wave functions (set II) with corresponding eigenenergies E, which fall outside and inside the range of $(-2\kappa, 2\kappa)$, respectively. Note that this range defines the energy band of the tight-binding lattice in the absence of the Stark potential.

(3) The spectrum $E_\alpha^{(I)}$ of the high-energy wave functions is given by

$$E_\alpha^{(I)} = \pm 2\kappa \cosh\phi_\alpha, \tag{6}$$

where $\phi_\alpha > 0$ is the root of the transcendental equation [Fig. 1(b)],

$$\frac{\sinh\phi_\alpha \cosh(\phi_\alpha M)}{\sinh(M\phi_\alpha)} = \pm\frac{\alpha FM}{2\kappa}, \tag{7}$$

and $\alpha = \pm1, \pm2, \pm3, \ldots$ is an arbitrary integer.

(4) The spectrum $E_{\alpha,\rho}^{(II)}$ of the low-energy wave functions is given by

$$E_{\alpha,\rho}^{(II)} = 2\kappa \cos\theta_{\alpha,\rho}, \tag{8}$$

where $0 \leqslant \theta_{\alpha,\rho} \leqslant \pi$ are the $(M-1)$ roots of the transcendental equation [Fig. 1(b)],

$$\frac{\sin\theta_{\alpha,\rho}\cos(\theta_{\alpha,\rho}M)}{\sin(M\theta_{\alpha,\rho})} = \frac{\alpha FM}{2\kappa}, \tag{9}$$

$\alpha = 0, \pm1, \pm2, \pm3, \ldots$ is an arbitrary integer and $\rho = 1, 2, \ldots, M-1$ labels the root number of Eq. (9) for a given value of α [see Fig. 1(c)].

(5) At the lattice sites $nM = 0, \pm M, \pm2M, \pm3M, \ldots$, i.e., where the potential is nonvanishing, the localized wave functions for both low-energy and high-energy branches, are given in terms of Bessel functions of first kind, namely,

$$\psi_{nM}^{(\alpha)} = (-1)^{n-\alpha} J_{n-\alpha}(\Gamma), \tag{10}$$

where we have set

$$\Gamma = \Gamma_\alpha = \frac{2\kappa}{FM}\frac{\sinh\phi_\alpha}{\sinh(M\phi_\alpha)} \tag{11}$$

for the high-energy wave functions, and

$$\Gamma = \Gamma_{\alpha,\rho} = \frac{2\kappa}{FM}\frac{\sin\theta_{\alpha,\rho}}{\sin(M\theta_{\alpha,\rho})} \tag{12}$$

for the low-energy wave functions ($\alpha = 0, \pm1, \pm2, \ldots$, $\rho = 1, 2, ..., M-1$). The wave functions at the sites $(nM+1)$, i.e., where the potential vanishes, are given by

$$\psi_{nM+1}^{(\alpha)} = (-1)^{n-\alpha}\frac{\sin[(M-1)\omega]J_{n-\alpha}(\Gamma) - \sin\omega J_{n+1-\alpha}(\Gamma)}{\sin(M\omega)}, \tag{13}$$

with $\omega = i\phi_\alpha, i\phi_\alpha + \pi$ for the high-energy wave functions and $\omega = \theta_{\alpha,\rho}$ for the low-energy wave functions.

Comments.

(i) The infinitely countable set of energies $E_{\alpha,\rho}^{(II)}$ of the low-energy wave functions are embedded in the interval $(-2\kappa, 2\kappa)$ and condense toward the isolated points E_σ of extended states [Eq. (4)] as $\alpha \to \pm\infty$ because $\sin(M\theta_{\alpha,\rho}) \sim 0$. Therefore, set of energies $E_{\alpha,\rho}^{(II)}$ form $(M-1)$ narrow "bands" centered at the around the energies E_σ.

(ii) As $E_{\alpha,\rho}^{(II)}$ approaches the isolated points E_σ of extended states, from Eqs. (10) and (13), one has $|\psi_{Mn}^{(\alpha)}/\psi_{nM+1}^{(\alpha)}| \ll 1$, i.e., the wave functions with energies close to the isolated points of extended states have negligible excitations at the lattices sites $0, \pm M, \pm2M, \pm3M, \ldots$ where the potential is nonvanishing.

(iii) The wave function $\psi_n^{(\alpha)}$ is centered at around $n = M\alpha$. Owing to the properties of the Bessel functions, the spatial size w of the wave function can be estimated from the relation $w \sim 2\Gamma M$ and, thus, from Eq. (12), it follows that w diverges for the low-energy wave functions as $\alpha \to \pm\infty$, i.e., when the eigenenergy $E_{\alpha,\rho}^{(II)}$ approaches one of the points E_σ of the energy spectrum.

(iv) The energies $E_\alpha^{(I)}$ of the high-energy wave functions fall outside the range of $(-2\kappa, 2\kappa)$, and in the limit $\alpha \to \pm\infty$, one has $E_\alpha^{(I)} \simeq \alpha FM$, and the corresponding wave function is tightly confined at the lattice site $n = \alpha$. This means that the set of energies $E_\alpha^{(I)}$ forms an almost equally spaced Wannier-Stark ladder.

(v) A corollary of the theorem is that the mosaic Wannier-Stark Hamiltonian does not show, strictly speaking, any mobility edge, although the low-energy localized eigenstates become more and more extended in space as their energy approaches the accumulation points E_σ defined by Eq. (4).

Proof. To prove the main theorem, let us write Eq. (1) in the dynamical system form

$$\begin{pmatrix}\psi_{n+1}\\ \psi_n\end{pmatrix} = \begin{pmatrix}\frac{E-V_n}{\kappa} & -1\\ 1 & 0\end{pmatrix}\begin{pmatrix}\psi_n\\ \psi_{n-1}\end{pmatrix}. \tag{14}$$

If we iterate Eq. (14) M times, starting from the sites $(\psi_{(n-1)M+1}, \psi_{(n-1)M})$ up to the sites (ψ_{nM+1}, ψ_{nM}), we obtain

$$\begin{pmatrix}\psi_{nM+1}\\ \psi_{nM}\end{pmatrix} = \begin{pmatrix}\frac{E-nMF}{\kappa} & -1\\ 1 & 0\end{pmatrix}\begin{pmatrix}\frac{E}{\kappa} & -1\\ 1 & 0\end{pmatrix}^{M-1} \times \begin{pmatrix}\psi_{(n-1)M+1}\\ \psi_{(n-1)M}\end{pmatrix}. \tag{15}$$

Note that the sites ψ_{nM+1} and $\psi_{(n-1)M+1}$ where the potential vanishes are just right next to the sites with the nonzero potential. Unlike previous works [41,43], we do not use Lyapunov exponent analysis and Avila's global theory to determine the localization properties of the wave functions. In fact, whereas, Lyapunov exponent analysis can be safely applied to quasiperiodic or disordered models displaying Anderson-like localization where the existence of Lyapunov exponent $L(E) \geqslant 0$ can be proven for any eigenstate (extended, critical, or localized with an exponential localization), it cannot be applied to wave functions with a higher than exponential localization, which is the case of the Wannier-Stark localization. Rather, we provide an exact analytical solution to the dynamical system Eq. (15). For the properties of 2×2 unimodular matrices, one can write

$$\begin{pmatrix}\frac{E}{\kappa} & -1\\ 1 & 0\end{pmatrix}^{M-1} = \begin{pmatrix}\frac{\sin(M\omega)}{\sin\omega} & -\frac{\sin[(M-1)\omega)]}{\sin\omega}\\ \frac{\sin[(M-1)\omega)]}{\sin\omega} & -\frac{\sin[(M-2)\omega)]}{\sin\omega}\end{pmatrix}, \tag{16}$$

where the complex angle ω is defined by the relation,

$$\cos\,\omega = \frac{E}{2\kappa}. \tag{17}$$

After letting

$$\varphi_n \equiv \psi_{nM}, \quad \xi_n \equiv \psi_{nM+1} \tag{18}$$

from Eqs. (15) and (16), one obtains

$$\xi_n = S_{11}\xi_{n-1} + S_{12}\varphi_{n-1}, \tag{19}$$

$$\varphi_n = S_{21}\xi_{n-1} + S_{22}\varphi_{n-1}, \tag{20}$$

where we have set

$$\begin{aligned} S_{11} &= \frac{\sin(M\omega)}{\sin\,\omega}\left(\frac{E}{\kappa} - \frac{FM}{\kappa}n\right) - \frac{\sin[(M-1)\omega]}{\sin\,\omega} \\ S_{12} &= -\frac{\sin[(M-1)\omega]}{\sin\,\omega}\left(\frac{E}{\kappa} - \frac{FM}{\kappa}n\right) + \frac{\sin[(M-2)\omega]}{\sin\,\omega} \\ S_{21} &= \frac{\sin(M\omega)}{\sin\,\omega} \\ S_{22} &= -\frac{\sin[(M-1)\omega]}{\sin\,\omega}. \end{aligned} \tag{21}$$

Taking into account that $\det S = S_{11}S_{22} - S_{12}S_{21} = 1$, eliminating form Eqs. (19) and (20) the variables ξ_n one obtains the following second-order difference equation for the amplitudes φ_n:

$$\varphi_{n+1} + \varphi_{n-1} = (A - Bn)\varphi_n, \tag{22}$$

where we have set

$$A \equiv 2\cos(M\omega), \tag{23}$$

$$B \equiv \frac{FM}{\kappa}\frac{\sin(M\omega)}{\sin\,\omega}. \tag{24}$$

The spectral problem on the infinite lattice defined by Eq. (22) is the usual Wannier-Stark problem on a tight-binding lattice but with energy-dependent DC force, which is solved in terms of J_n Bessel functions of first kind. Here, we give a direct solution to the spectral problem exploiting a recursive identity of Bessel functions J_n; a different approach based on a spectral method could be also used.

Let us first assume $B \neq 0$, i.e., $\sin(M\omega)/\sin\,\omega \neq 0$. Using the recursive relation of $J_n(x)$ Bessel functions,

$$J_{n+1}(x) + J_{n-1}(x) = \frac{2n}{x}J_n(x), \tag{25}$$

the set of solutions to Eq. (22), which do not diverge as $n \to \pm\infty$, is given by

$$\varphi_n^{(\alpha)} = (-1)^{n-\alpha}J_{n-\alpha}(\Gamma), \tag{26}$$

where $\alpha = 0, \pm1, \pm2, \pm3\cdots$ is an arbitrary integer number,

$$\Gamma = \frac{2\kappa}{FM}\frac{\sin\,\omega}{\sin(M\omega)}, \tag{27}$$

and ω is any root of the transcendental equation,

$$\sin\,\omega\frac{\cos(M\omega)}{\sin(M\omega)} = \alpha\frac{FM}{2\kappa}. \tag{28}$$

Since the energy E is real and it is related to the complex angle ω by the relation $E = 2\kappa\,\cos\,\omega$ [Eq. (17)], Eq. (28) can be satisfied by letting either $\omega = i\phi$, $\omega = i\phi + \pi$, or $\omega = \theta$, with θ and ϕ real numbers. The first two cases, $\omega = i\phi$ or $\omega = i\phi + \pi$, yield the high-energy wave functions with energies $E_\alpha^{(I)}$ defined by Eqs. (6) and (7) with the $+$ and $-$ signs in the equations corresponding to $\omega = i\phi$ and $\omega = i\phi + \pi$, respectively. On the other hand, the last case of $\omega = \theta$ yields the low-energy wave functions with energies $E_\alpha^{(II)}$ defined by Eqs. (8) and (9). In all cases, the corresponding wave functions are given in terms of Bessel functions as in Eqs. (10)–(12). Finally, using Eq. (20) the wave functions $\psi_{nM+1}^{(\alpha)}$ at sites $nM+1$ are obtained from the relation,

$$\psi_{nM+1}^{(\alpha)} = \xi_n = \frac{\varphi_{n+1} - S_{22}\varphi_n}{S_{21}}, \tag{29}$$

which yields Eq. (13). For $M \geqslant 3$, the wave-function amplitudes $\psi_n^{(\alpha)}$ at the other lattice sites $Mn + l$ with $l = 2, 3, \ldots M-1$ if needed, can be obtained by the recursive relation (14).

Let us finally assume $B = 0$ in Eq. (22), i.e., $\sin(M\omega) = 0$ with $\omega \neq 0, \pi$, which is satisfied by letting $\omega = \sigma\pi/M$ for $\sigma = 1, 2, \ldots, M-1$. Correspondingly, the eigenenergies are $E_\sigma = 2\kappa\,\cos(\pi\sigma/M)$. In this case, $S_{21} = 0$, whereas, $S_{11}, S_{12} \neq 0$ so that to avoid divergences as $n \to \pm\infty$ of the solution to Eqs. (19) and (20), one necessarily must have $\varphi_n = 0$, i.e., the wave-function ψ_l vanishes identically at the lattice sites $l = nM = 0, \pm M, \pm 2M, \pm 3M, \ldots$ where the potential V_l is nonvanishing. This means that the wave-function ψ_l is also an eigenfunction of the tight-binding lattice without any potential with eigenenergy E_σ. Such solutions are the well-known Bloch waves given by Eq. (5), which identically vanish at the lattice sites $0, \pm M, \pm 2M, \pm 3M, \ldots$. This concludes the proof of statements (1)–(5) given above. The comments (i)–(v) are simple corollaries of the main theorem. ■

It should be mentioned that the condensation of the countably infinite set of low-energies $E_{\alpha,\rho}^{(II)}$ toward the $(M-1)$ points E_σ leads to a divergence in the density of states at $E = E_\sigma$, which is similar to the singular behavior found in the Dyson one-dimensional random hopping model (see, e.g., Refs. [49–53] and references therein). This model shows pure nearest-neighbor hopping disorder with no on-site potential, and, hence, it is also known as the off-diagonal disorder model. It displays sublattice (chiral) symmetry with an exact pairing of states in the spectrum. Under some weak conditions on the probability density distribution of the off-diagonal disorder, the energy spectrum is pure point and the density of states shows a diverging behavior near $E = 0$, which is also accompanied by a divergence in the localization length, i.e., vanishing of the Lyapunov exponent. Unlike the mosaic Wannier-Stark model studied in this paper, in the Dyson random hopping model the eigenstate at zero energy is not conventionally extended rather it is subexponentially localized with a decay behavior $\psi_n \sim \exp(-\gamma\sqrt{|n|})$ of the wave function [51–53]. Also, all other localized states show an exponential (Anderson-like) localization with a finite Lyapunov exponent, whereas, in the mosaic Wannier-Stark model considered in the present paper, the eigenfunctions show a higher than exponential localization.

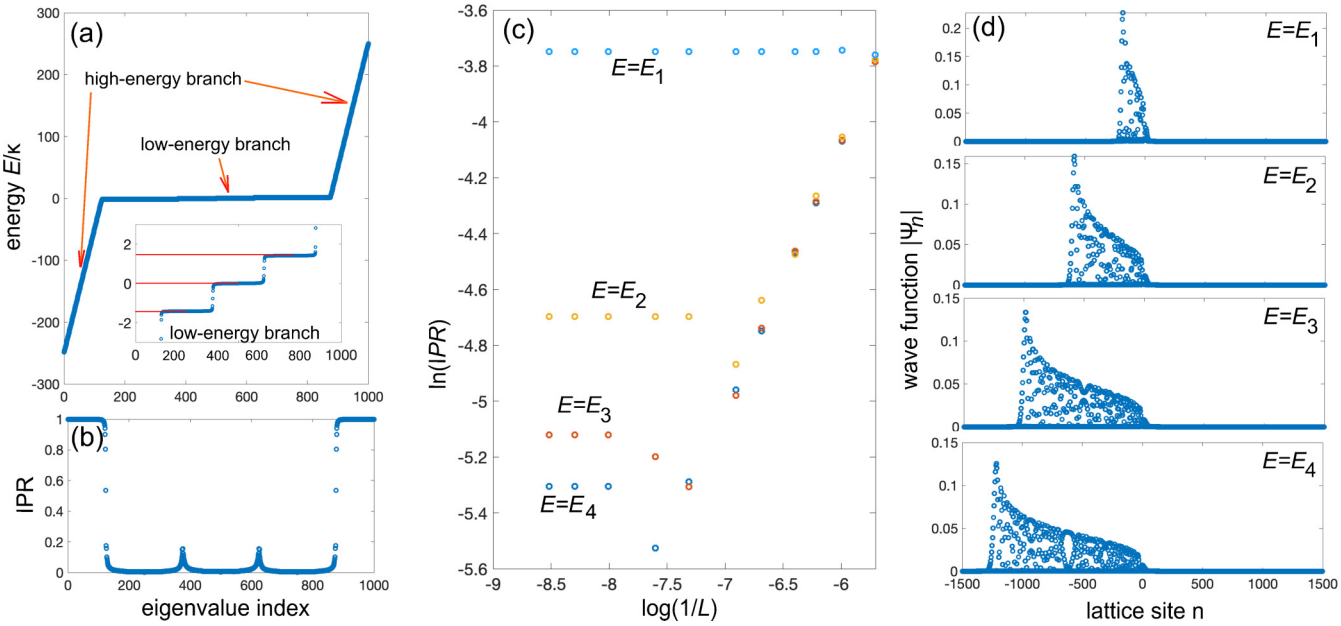

FIG. 2. (a) Numerically computed energy in a lattice of size $L = 1000$ with open boundary conditions for parameter values $M = 4$ and $F/\kappa = 0.5$. The inset shows an enlargement of the energy spectrum corresponding to the low-energy branch $E_\alpha^{(II)}$, clearly showing that the eigenenergies condensate toward the $(M-1) = 3$ values of $0, \pm\sqrt{2}\kappa$, corresponding to the energies of the isolated extended states (horizontal red curves). (b) The IPR of the corresponding wave functions. Note that the IPR of the high-energy wave functions is very close to one, indicating strong localization, whereas, the IPR of the low-energy wave functions is small, indicating a low degree of localization. Note also that the two cusps visible in the IPR plot occur at the transition energies that separate the energy plateaus displayed in the inset of panel (a). (c) Behavior of ln(IPR) versus $\ln(1/L)$ for four low-energy wave functions with energies E_{1-4} that approach the zero energy of the extended state($E_1 = 0.020\kappa$, $E_2 = 0.0067\kappa$, $E_3 = 0.0040\kappa$, and $E_4 = 0.0032\kappa$). The slopes of the curves at $L \to \infty$ give the fractal dimension β of the wave functions, with $\beta = 1$ for extended states, $0 < \beta < 1$ for critical states and $\beta = 0$ for localized states. Note that all wave functions are localized, even though the IPR is very small. A weakly localized state differs from a critical or a fully extended state because the IPR settles down to a constant (albeit small) value as $L \to \infty$, and the fractal dimension β correspondingly vanishes. (d) Shape of the wave-function amplitudes $|\psi_n|$ corresponding to the four energies in a lattice of size $L = 3000$. Note that the wave functions are very weakly localized, extending over several hundreds of lattice sites.

III. NUMERICAL RESULTS AND COMMENTS

To illustrate and support the analytical results given in the previous section, we present some numerical results of energy spectra and localization properties of corresponding wave functions. The results are obtained by diagonalization of the matrix Hamiltonian $\mathcal{H}$ (EIG MatLab solver) assuming a finite lattice of large size L with open boundary conditions. We also comment on the pseudomobility edges that have been introduced in previous works [41–43], where the inverse participation ratio (IPR) was used to discriminate between localized and extended states. For a wave function normalized such that $\sum_{n=1}^{L} |\psi_n^{(\alpha)}|^2 = 1$, the IPR is defined by the relation,

$$\mathrm{IPR}_\alpha = \sum_{n=1}^{L} \left|\psi_n^{(\alpha)}\right|^4. \tag{30}$$

The IPR of an extended state takes a small value and scales as L^{-1}, hence, vanishing in the thermodynamic limit $L \to \infty$, whereas, it remains finite for a localized state. In the mosaic Wannier-Stark lattice of finite size L, we expect $\sim L/M$ eigenstates belonging to the high-energy branch I, and the other $L(1-1/M)$ eigenstates belonging to the low-energy branch II. In fact, the eigenstates belonging to the high-energy branch have their excitations tightly confined in almost one site of the lattice where the potential is nonvanishing. Since the fraction of sites in the lattice where the potential is nonvanishing is given by $1/M$ for large L, we expect to have $\sim L/M$ tightly localized wave functions belonging to the high-energy branch. In a lattice of finite (albeit large) size L, the analytical form of the high-energy eigenstates and corresponding eigenenergies are not substantially modified by edge effects since the wave functions are tightly localized in the bulk (apart for few wave functions localized at the lattice boundaries). For the high-energy branch, the eigenenergies are, thus, given again by Eqs. (8) and (9) to a high degree of approximation where the index α varies in the range of $(-L/2M, L/2M)$ with $\alpha \neq 0$. On the other hand, a large fraction of eigenstates belonging to the low-energy branch are so extended to reach the lattice edges so that in this case, the exact form of the wave functions cannot be given in an exact form and Eqs. (10) and (13) cannot be used anymore when the wave functions reach the lattice edges.

Figure 2(a) shows, as an example, the numerically computed energy spectrum for $M = 4$ and for $F/\kappa = 0.5$ in a lattice of size $L = 1000$. The corresponding IPR of the wave functions is shown in Fig. 2(b). The energy spectrum in Fig. 2(a) clearly shows that, besides high-energy eigenstates, a large fraction of the wave functions, namely, $\sim L(1-1/M)$ wave functions, have their energy in three narrow regions [see the insets in Fig. 2(a)] that condensate toward the $(M-1) =$

3 energies $E_\sigma = 0, \pm\sqrt{2}\kappa$ of extended states. As shown in Fig. 2(b), the IPR of the high-energy wave functions is very close to one, indicating a tight localization of the wave functions. On the other hand, the IPR of the low-energy wave functions is small, reaching a value down to $\sim$0.005 close to the three energies E_σ. However, a small value of the IPR alone does not necessarily mean that the wave function is an extended or critical state, it just tells us that the excitation spreads over several sites of the lattice. The nature of the function $\psi_n^{(\alpha)}$ is at best captured by looking at its fractal dimension β_α, which is defined by (see, e.g., Refs. [35,36,54])

$$\beta_\alpha = \lim_{L\to\infty} \frac{\ln IPR_\alpha}{\ln(1/L)}. \tag{31}$$

For a localized wave function, one has $\beta_\alpha = 0$, for an extended wave function, one has $\beta_\alpha = 1$, whereas, for a critical wave function, one has $0 < \beta_\alpha < 1$. In our example, the energy spectrum contains $(M-1) = 3$ fully extended states at the energies $E_\sigma = 0, \pm\sqrt{2}\kappa$, and for such states, one clearly has $\beta = 1$. In Fig. 2(c), we show the numerically computed behavior of ln(IPR) versus $\ln(1/L)$ for four wave functions with energies $E_1 = 0.020\kappa$, $E_2 = 0.0067\kappa$, $E_3 = 0.0040\kappa$, $E_4 = 0.0032\kappa$ that approach the zero-energy value of one of the three extended states. The figure clearly shows that, for a fixed energy (albeit very close to zero) the behavior of ln(IPR) becomes independent of $\ln(1/L)$ for large enough system size L, indicating that the slope β vanishes, and the wave function is not strictly an extended state, although the excitation can spread over many sites of the lattice. As an example, in Fig. 2(d), we plot the wave function amplitudes for the four energies in a lattice of size $L = 3000$, clearly showing that, even though the excitation spreads over several hundreds of sites in the lattice, with a very small IPR, the wave function asymptotically decays toward zero and, thus, belongs to the point spectrum of the Hamiltonian in the $L \to \infty$ limit. The α indices for the wave functions depicted in Fig. 2(d) can be calculated from the simple relation $\alpha \simeq -4\kappa^2/(M^2EF)$, where E is the energy of the wave function close to the condensation point $E_0 = 0$. For example, for the wave function with energy $E = E_1 = 0.020\kappa$ one has $\alpha = -25$. We checked that the wave function profiles obtained from the numerical matrix diagonalization match with an excellent accuracy the analytical forms given in terms of Bessel functions [Eqs. (10) and (13)].

In systems with a finite size L, a relevant number of eigenstates with energies very close to the $(M-1)$ values E_σ, are, nevertheless, extended over the entire lattice and can be, thus, considered as extended states in a broad sense. The mobility edges, i.e., the energies separating such wave functions extended over the entire size L of the lattice from localized wave functions, clearly shrink toward the $(M-1)$ energies E_σ in a system of large size L, indicating that the spectral extent (but not the number of wave functions) of such extended states shrink to zero in the $L \to \infty$ limit, according to the Simon-Spencer theorem [48]. This result is clearly at odds with the results presented in Ref. [41]. However, one can retrieve the results of Ref. [41], and, in particular, the form of pseudomobility edges, introducing the notion of an 'extended state' in a weaker sense by classifying a wave function as an extended state whenever its IPR is smaller than an assigned (small) number ϵ, and a localized state when its IPR is larger than ϵ. Using the property of Bessel functions that $J_n(\Gamma)$ extends over $\sim 2|\Gamma|$ sites of the lattice, we can roughly estimate the size w of a narrow-energy wave function using Eq. (27), i.e.,

$$w \sim 2M|\Gamma| = \left|\frac{4\kappa}{F}\frac{\sin\theta}{\sin(M\theta)}\right|, \tag{32}$$

where angle θ is related to energy E via the relation $E = 2\kappa\cos\theta$. For a wave function with excitation uniformly distributed over w sites of the lattice, the IPR is clearly estimated by the relation,

$$\text{IPR} \sim 1/w, \tag{33}$$

and, thus, from Eqs. (32) and (33), one obtains

$$\text{IPR} \sim \left|\frac{F}{4\kappa}\frac{\sin(M\theta)}{\sin\theta}\right|. \tag{34}$$

The pseudomobility edges are, thus, obtained from the relation $\text{IPR} = \epsilon$, i.e.,

$$\left|\frac{F}{4\kappa}\frac{\sin(M\theta)}{\sin\theta}\right| = \epsilon. \tag{35}$$

If we assume $\epsilon = 1/2$ and let $a_M \equiv \sin(M\theta)/\sin\theta$, the pseudo-mobility edges are, thus, defined by the relation,

$$\left|\frac{F}{\kappa}a_M\right| = 2, \tag{36}$$

which is precisely the result obtained in Ref. [41] for the mobility edges [see Eq. (11) of this reference].

IV. CONCLUSIONS

To summarize, we reported on the exact analytical solution of the spectral problem of the mosaic Wannier-Stark Hamiltonian, a tight-binding model, which has been introduced in recent works [41–43] as an example of a disorder-free system displaying mobility edges, separating localized and extended states. This result looks quite surprising since so far all known one-dimensional models displaying mobility edges require some kind of (incommensurate) disorder. Our results indicate that for the mosaic Wannier-Stark Hamiltonian, strictly speaking, there are not mobility edges, separating extended and localized states. Specifically, we proved that the energy spectrum is almost pure point with all the wave functions displaying a higher than exponential localization, typical of Wannier-Stark localization with the exception of $(M-1)$-isolated extended states. The energy spectrum comprises two sets of countably infinite number of localized states, the low-energy and high-energy wave functions. Althoughe the high-energy wave functions are tightly localized, the low-energy wave functions are weakly localized, and they become more and more extended as their energies approach the energies of the isolated extended states.

ACKNOWLEDGMENTS

I knowledge the Spanish State Research Agency, through the Severo Ochoa and Maria de Maeztu Program for Centers and Units of Excellence in R&D (Grant No. MDM-2017-0711).

[1] P. W. Anderson, Absence of diffusion in certain random lattices, Phys. Rev. **109**, 1492 (1958).

[2] A. Lagendijk, B. van Tiggelen, and D. S. Wiersma, Fifty years of Anderson localization, Phys. Today **62**(8), 24 (2009).

[3] E. Abrahams, *50 Years of Anderson Localization* (World Scientific Publishing, Singapore, 2010).

[4] F. Evers and A. D. Mirlin, Anderson transitions, Rev. Mod. Phys. **80**, 1355 (2008),

[5] M. Segev, Y. Silberberg, and D. N. Christodoulides, Anderson localization of light, Nat. Photonics **7**, 197 (2013).

[6] T. Schwartz, G. Bartal, S. Fishman, and M. Segev, Transport and Anderson localization in disordered two-dimensional photonic lattices, Nature (London) **446**, 52 (2007).

[7] Y. Lahini, A. Avidan, F. Pozzi, M. Sorel, R. Morandotti, D. N. Christodoulides, and Y. Silberberg, Anderson Localization and Nonlinearity in One-Dimensional Disordered Photonic Lattices, Phys. Rev. Lett. **100**, 013906 (2008).

[8] H. Hu, A. Strybulevych, J. H. Page, S. E. Skipetrov, and B. A. van Tiggelen, Localization of ultrasound in a three-dimensional elastic network, Nat. Phys. **4**, 945 (2008).

[9] G. Roati, C. D'Errico, L. Fallani, M. Fattori, C. Fort, M. Zaccanti, G. Modugno, M. Modugno, and M. Inguscio, Anderson localization of a non-interacting Bose-Einstein condensate, Nature (London) **453**, 895 (2008).

[10] J. Billy, V. Josse, Z. Zuo, A. Bernard, B. Hambrecht, P. Lugan, D. Clément, L. Sanchez-Palencia, P. Bouyer, and A. Aspect, Direct observation of Anderson localization of matter waves in a controlled disorder, Nature (London) **453**, 891 (2008).

[11] S. S. Kondov, W. R. McGehee, J. J. Zirbel, and B. DeMarco, Three-dimensional Anderson localization of ultracold matter, Science **334**, 66 (2011).

[12] F. Jendrzejewski, A. Bernard, K. Müller, P. Cheinet, V. Josse, M. Piraud, L. Pezzé, L. Sanchez-Palencia, A. Aspect, and P. Bouyer, Three-dimensional localization of ultracold atoms in an optical disordered potential, Nat. Phys. **8**, 398 (2012).

[13] G. Semeghini, M. Landini, P. Castilho, S. Roy, G. Spagnolli, A. Trenkwalder, M. Fattori, M. Inguscio, and G. Modugno, Measurement of the mobility edge for 3D Anderson localization, Nat. Phys. **11**, 554 (2015).

[14] I. V. Gornyi, A. D. Mirlin, and D. G. Polyakov, Interacting Electrons in Disordered Wires: Anderson Localization and Low-T Transport, Phys. Rev. Lett. **95**, 206603 (2005).

[15] E. Abrahams, P. W. Anderson, D. C. Licciardello, and T. V. Ramakrishnan, Scaling Theory of Localization: Absence of Quantum Diffusion in Two Dimensions, Phys. Rev. Lett. **42**, 673 (1979).

[16] N. Mott, The mobility edge since 1967, J. Phys. C: Solid State Phys. **20**, 3075 (1987).

[17] L. Sanchez-Palencia, Ultracold gases: At the edge of mobility, Nat. Phys. **11**, 525 (2015)

[18] S. Das Sarma, S. He, and X. C. Xie, Mobility Edge in a Model One-Dimensional Potential, Phys. Rev. Lett. **61**, 2144 (1988)

[19] H. Hiramoto and M. Kohmoto, New Localization in a Quasiperiodic System, Phys. Rev. Lett. **62**, 2714 (1989).

[20] J. Biddle and S. Das Sarma, Predicted Mobility Edges in One-Dimensional Incommensurate Optical Lattices: An Exactly Solvable Model of Anderson Localization, Phys. Rev. Lett. **104**, 070601 (2010).

[21] S. Ganeshan, J. H. Pixley, and S. Das Sarma, Nearest Neighbor Tight Binding Models with an Exact Mobility Edge in One Dimension, Phys. Rev. Lett. **114**, 146601 (2015).

[22] T. Liu, H. Guo, Y. Pu, and S. Longhi, Generalized Aubry-André self-duality and Mobility edges in non-Hermitian quasiperiodic lattices, Phys. Rev. B **102**, 024205 (2020).

[23] S. Das Sarma, Song He, and X. C. Xie, Localization, mobility edges, and metal-insulator transition in a class of one-dimensional slowly varying deterministic potentials, Phys. Rev. B **41**, 5544 (1990).

[24] H. Yao, H. Khouldi, L. Bresque, and L. Sanchez-Palencia, Critical Behavior and Fractality in Shallow One-Dimensional Quasiperiodic Potentials, Phys. Rev. Lett. **123**, 070405 (2019).

[25] H. Yao, T. Giamarchi, and L. Sanchez-Palencia, Lieb-Liniger Bosons in a Shallow Quasiperiodic Potential: Bose Glass Phase and Fractal Mott Lobes, Phys. Rev. Lett. **125**, 060401 (2020).

[26] D. J. Boers, B. Goedeke, D. Hinrichs, and M. Holthaus, Mobility edges in bichromatic optical lattices, Phys. Rev. A **75**, 063404 (2007).

[27] H. P. Lüschen, S. Scherg, T. Kohlert, M. Schreiber, P. Bordia, X. Li, S. Das Sarma, and I. Bloch, Single-Particle Mobility Edge in a One-Dimensional Quasiperiodic Optical Lattice, Phys. Rev. Lett. **120**, 160404 (2018).

[28] Z. Xu, H. Huangfu, Y. Zhang, and S. Chen, Dynamical observation of mobility edges in one-dimensional incommensurate optical lattices, New J. Phys. **22**, 013036 (2020).

[29] J. D. Bodyfelt, D. Leykam, C. Danieli, X. Yu, and S. Flach, Flatbands under Correlated Perturbations, Phys. Rev. Lett. **113**, 236403 (2014).

[30] Y. Wang, X. Xia, L. Zhang, H. Yao, S. Chen, J. You, Q. Zhou, and X. Liu, One Dimensional Quasiperiodic Mosaic Lattice with Exact Mobility Edges, Phys. Rev. Lett. **125**, 196604 (2020).

[31] Q. Tang and Y. He, Mobility edges in one-dimensional models with quasi-periodic disorder, J. Phys.: Condens. Matter **33**, 185505 (2021).

[32] Y. Wang, X. Xia, J. You, Z. Zheng, and Q. Zhou, Exact mobility edges for 1D quasiperiodic models, Commun. Math. Phys. **401**, 2521 (2023).

[33] S. Jitomirskaya and F. Yang, Singular Continuous Spectrum for Singular Potentials, Commun. Math. Phys. **351**, 1127 (2017).

[34] F. Yang and S. Zhang, Singular continuous spectrum and generic full spectral/packing dimension for unbounded quasiperiodic Schrödinger operators, Ann. Henri Poincaré **20**, 2481 (2019).

[35] T. Liu, X. Xia, S. Longhi, and L. Sanchez-Palencia, Anomalous mobility edges in one-dimensional quasiperiodic models, SciPost Phys. **12**, 027 (2022).

[36] Y.-C. Zhang and Y.-Y. Zhang, Lyapunov exponent, mobility edges, and critical region in the generalized Aubry-Andre model with an unbounded quasiperiodic potential, Phys. Rev. B **105**, 174206 (2022).

[37] T. Xiao, D. Xie, Z. Dong, T. Chen, W. Yi, and B. Yan, Observation of topological phase with critical localization in a quasi-periodic lattice, Sci. Bull. **66**, 2175 (2021),

[38] Y. Wang, L. Zhang, W. Sun, T.-F. J. Poon, and X.-J. Liu, Quantum phase with coexisting localized, extended, and critical zones, Phys. Rev. B **106**, L140203 (2022).

[39] T. Shimasaki, M. Prichard, H. E. Kondakci, J. Pagett, Y. Bai, P. Dotti, A. Cao, T.-C. Lu, T. Grover, and D. M. Weld, Anoma-

lous localization and multifractality in a kicked quasicrystal, arXiv:2203.09442.

[40] X. Lin, X. Chen, G.-C. Guo, and M. Gong, The general approach to the critical phase with coupled quasiperiodic chains, arXiv:2209.03060.

[41] D. Dwiputra and F. P. Zen, Single-particle mobility edge without disorder, Phys. Rev. B **105**, L081110 (2022).

[42] J. Gao, I. M. Khaymovich, A. Iovan, X.-W. Wang, G. Krishna, Z.-S. Xu, E. Tortumlu, A. V. Balatsky, V. Zwiller, and A. W. Elshaari, Observation of Wannier-Stark ladder beyond mobility edge in disorder-free mosaic lattices, arXiv:2306.10831.

[43] R. Qi, J. Cao, and X.-P. Jiang, Localization and mobility edges in non-Hermitian disorder-free lattices, arXiv:2306.03807.

[44] G. H. Wannier, Dynamics of band electrons in electric and magnetic fields, Rev. Mod. Phys. **34**, 645 (1962).

[45] H. Fukuyama, R. A. Bari, and H. C. Fogedby, Tightly bound electrons in a uniform electric field, Phys. Rev. B **8**, 5579 (1973).

[46] D. Emin and C. F. Hart, Existence of Wannier-Stark localization, Phys. Rev. B **36**, 7353 (1987).

[47] T. Hartmann, F. Keck, H. J. Korsch, and S. Mossmann, Dynamics of Bloch oscillations, New J. Phys. **6**, 2 (2004).

[48] B. Simon and T. Spencer, Trace class perturbations and the absence of absolutely continuous spectra, Commun. Math. Phys. **125**, 113 (1989).

[49] G. Theodorou and M. H. Cohen, Extended states in a one-dimensional system with off-diagonal disorder, Phys. Rev. B **13**, 4597 (1976).

[50] T. P. Eggarter and R. Riedinger, Singular behavior of tight-binding chains with off-diagonal disorder, Phys. Rev. B **18**, 569 (1978).

[51] L. Fleishman and D. C. Licciardello, Fluctuations and localization in one dimension, J. Phys. C: Solid State Phys. **10**, L125 (1977).

[52] C. M. Soukoulis and E. N. Economou, Off-diagonal disorder in one-dimensional systems, Phys. Rev. B **24**, 5698 (1981).

[53] A. Krishna and R. N. Bhatt, Beyond universal behavior in the one-dimensional chain with random nearest-neighbor hopping, Phys. Rev. B **101**, 224203 (2020).

[54] M. Schreiber, Fractal eigenstates in disordered systems, Physica A **167**, 188 (1990).